

The Rovibrational Spectrum and Structure of the Weakly Bound CO₂–CS₂ Complex

C. C. Dutton,[†] D. A. Dows,[†] R. Eikey,^{†,‡} S. Evans,^{†,§} and R. A. Beaudet^{*,†}

Department of Chemistry, University of Southern California, University Park, Los Angeles, California 90089-0482

Received: January 23, 1998; In Final Form: March 27, 1998

The rovibrational spectrum of the weakly bound complex CO₂–CS₂ was observed by exciting the asymmetric stretch of the CO₂ moiety near 2349 cm⁻¹. The complex was formed by the supersonic expansion of a 1:2 mixture of CO₂ and CS₂ in helium and had a nonplanar X-shaped structure. The intermolecular distance is 3.392 Å with a dihedral angle of 90°. The band center is located at 2346.5448 cm⁻¹, with ground-state rotational constants of $A'' = 0.08590$ cm⁻¹, $B'' = 0.04634$ cm⁻¹, and $C'' = 0.03546$ cm⁻¹ and centrifugal distortion constants of $D_j'' = -1.37 \times 10^{-7}$ cm⁻¹, $D_k'' = 1.06 \times 10^{-6}$ cm⁻¹, and $D_{jk}'' = -1.01 \times 10^{-6}$ cm⁻¹. The excited-state constants are similar to the ground-state constants. A portion of the potential energy surface was modeled through the use of a Buckingham atom–atom potential and a quadrupole–quadrupole electrostatic potential. Calculations for the CO₂–CS₂ and (CO₂)₂ complexes produced structures in agreement with experimental results. Although the CO₂–CS₂ configuration is controlled by the quadrupole–quadrupole interactions, the atom–atom interactions predominantly determine the energy of the dimer. Because the magnitude of the CS₂ quadrupole was increased in the electrostatic potential, the structure shifted from nonplanar X-shaped to a planar parallel configuration.

Introduction

The molecular structures of weakly bound complexes of CO₂ have been studied extensively by pure rotational and rovibrational spectroscopy. Carbon dioxide forms complexes with a wide range of partners, both polar and nonpolar. Because CO₂ is nonpolar, its large quadrupole moment must play an important role in the bonding.

These CO₂ complexes can assume various shapes, including linear, T-shaped, slipped parallel, and even some nonplanar configurations. A priori predictions of these structures have not always been successful and, in some cases, the experimental structures have not been easily explained after the fact. For example, HF and HCl form essentially linear complexes with CO₂,^{1–5} whereas HBr prefers a T-shaped structure,^{3,6} with the HBr axis parallel to the CO₂ axis. This structural change in the hydrogen halide series has been rationalized as a close interplay between the stability of the hydrogen bond that dominates in linear forms, and polarizability that prefers the T-shaped arrangement. Calculations done on this series by incorporating repulsion, dispersion, and electrostatic terms did not support the experimentally observed structures.⁷ The deviation was suggested to result from vibrational averaging effects. However, the trend is substantiated in the T-shaped CO₂–Rg complexes, where Rg represents He, Ne, Ar, Kr, and Xe. In this type of system, the structure is controlled by the interaction between the CO₂ quadrupole moment and the polarizability of the noble gas.^{8–12} Molecular bromine, like the heavier noble gases, is highly polarizable but also contains a sizable quadrupole moment. Unlike the CO₂–Rg complexes,

CO₂–Br₂ prefers a linear geometry.¹³ The CO₂–ClF complex was also found to have a linear geometry with the chlorine atom nearest the CO₂ oxygen.¹⁴ Though we have observed the rovibrational spectrum of the chlorine–carbon dioxide cluster, the complexity of the spectrum suggests there may be several structures or different species.

In CO₂–HCN, both the linear and the T-shaped form have been observed.^{15,16} In the linear configuration, the hydrogen forms a hydrogen bond with the CO₂ oxygen, similar to the smaller hydrogen halides. In the T-shaped configuration, the nitrogen atom is closest to the CO₂ carbon. Unlike the hydrogen halides, π orbitals can come into play. Thus, the bonding has been explained by a simple HOMO–LUMO model where the nitrogen lone pairs donate electron density to the empty CO₂ π^* orbitals. Ab initio calculations have indicated a third higher minimum at a slipped parallel structure; however, this structure has not been observed experimentally. The complex CO₂–N₂ is also T-shaped,¹⁷ with the molecular axis of N₂ directed along the leg of the T. Although the structure resembles CO₂–HCN, the bonding has been explained by electrostatic and dispersion interactions where the potential energy is more favorable with the nitrogen along the leg rather than on top of the T. In CO₂–CO, the lone pair on the CO carbon likewise interacts with the CO₂ carbon, resulting in a T-shaped cluster.¹⁸ The CO₂–H₂O dimer has a planar seesaw configuration,^{19,20} with a high barrier that hinders internal rotation (315 ± 70 cm⁻¹). The H₂O oxygen and CO₂ bond in a T-shaped fashion that can be attributed to an interaction between the oxygen lone pairs in H₂O and the partial positive charge on the carbon atom. Historically, a hydrogen-bonded complex was anticipated.

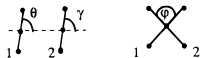
Carbon dioxide forms slipped parallel structures with itself,^{21–23} N₂O,²⁴ acetylene,^{25–27} and OCS,²⁸ a result that was not always expected. In planar H₂CO–CO₂, the CO-axis of formaldehyde is parallel to CO₂ with the H₂CO oxygen under the CO₂ carbon.²⁹

* To whom correspondence should be addressed.

[†] Department of Chemistry.

[‡] Present address: University of California at Los Angeles Department of Chemistry and Biochemistry, Los Angeles, CA 90095-1569.

[§] Present address: University of California at San Diego School of Medicine, San Diego, CA 92122.

TABLE 1: Comparison of Structures, Inertial Defect, and Asymmetry of Dimers Containing Linear Triatomics Closely Related to CO₂-CS₂^a


	CO ₂ -CO ₂ ^a	CO ₂ -OCS ^b	OCS-OCS ^c	N ₂ O-N ₂ O ^d	CO ₂ -N ₂ O ^e
<i>R</i> _{cm} (Å)	3.602	3.552	3.648	3.421	3.470
<i>θ</i> (deg)	58.0	68.9	85.2	61.2	60.1
<i>γ</i> (deg)	58.0	78.9	85.2	61.2	60.1
<i>φ</i> (deg)	0	0	0	0	0
Δ (amu Å ²)	+1.04	+0.93	+0.51	+0.67	+0.52
<i>κ</i>	-0.93	-0.77	-0.66	-0.92	-0.92
$\Delta\nu$ (cm ⁻¹)	+1.61	-	+9.81	-0.50	-0.30
structure	slip parallel	slip parallel	parallel	slip parallel	slip parallel

^a Dimer angles are defined below with monomers 1 and 2 corresponding to the first and second monomers listed in the table, respectively. $\Delta\nu$ is the shift in the dimer band center from the CO₂ monomer band center in dimers containing CO₂; N₂O in (N₂O)₂; and OCS in (OCS)₂. ^b References 18–20. ^c Reference 25; in this case, the monomers are slightly tilted from parallel because of the difference in size between the sulfur and oxygen atoms. ^d References 34 and 35. ^e Reference 33. ^f Reference 21.

Carbon dioxide also forms nonplanar dimers that are usually more complex spectroscopically. In the C₂H₄-CO₂ dimer,³⁰ CO₂ is parallel to the ethylene C-C axis and CO₂ lies directly above the ethylene plane. This structure is explained by the monomer units having large quadrupole moments of opposite sign. Both NH₃^{31,32} and H₂S³³ form essentially T-shaped complexes with CO₂ (discounting the hydrogens), with the electron lone pair(s) on nitrogen (sulfur) donating to the lowest unoccupied molecular orbital of carbon dioxide. In H₂S-CO₂, the H₂S molecule lies in a plane orthogonal to the S-CO₂ plane allowing for inversion of H₂S without changing the structure of the dimer.³⁴ Finally, SO₂-CO₂³⁵ was found to have an X-shaped structure, with the SO₂ oxygens pointing away from CO₂. This structure was rationalized by the interplay between the SO₂ dipole moment and the CO₂ quadrupole moment.

Given the wide array of dimer complexes involving CO₂, there appear to be no simple rules for predicting the experimental structure a priori. The linear triatomics OCS, CS₂, and N₂O are isoelectronic with and comparable in size to CO₂. Because N₂O and OCS possess a dipole moment whereas CO₂ and CS₂ do not, structural predictions of dimers involving these molecules should not necessarily lead to similar structures. However, the dimers (CO₂)₂, CO₂-OCS, CO₂-N₂O, (N₂O)₂,³⁶ and (OCS)₂^{37,38} all exhibit planar slipped parallel configurations (shown in Table 1). It was expected that CO₂-CS₂ would be planar.

In this paper, the structure of CO₂-CS₂ is shown to be X-shaped, a unique configuration for two nonpolar linear triatomics. This structure was not originally anticipated given the results of previous work. We have successfully modeled the nature of the bonding in the dimer through the use of atom-atom and electrostatic potentials where the parameters were taken from crystal data. The structure appears to be primarily controlled by the quadrupole-quadrupole interactions, whereas the energy of the dimer is primarily determined by the atom-atom interactions.

Experimental Section

The experimental apparatus has been described elsewhere,^{10,24} and only details relevant to this experiment will be discussed here. Carbon disulfide was obtained from Omni Solv (liquid chromatography grade, 0.004% H₂O residue). The CS₂ with a higher percentage water content significantly reduced the signal-to-noise ratio of CO₂-CS₂. The dimer was created by pre-mixing 0.8% CS₂ vapor with 0.4% prepurified CO₂ in high purity He. The gas mixture was expanded through a 12.5 cm

× 150 μm slit nozzle with a backing pressure of ~1.8 atm. The nozzle was pulsed at 3 Hz and remained open for ~1 ms. Two Pb salt diode lasers (Laser Photonics, Andover, MA) operating over a combined region of 2315–2375 cm⁻¹ were used to probe the CO₂ asymmetric stretch. Segments of the spectrum (~0.5 cm⁻¹) were recorded during single pulses and averaged 20–100 times, the number depending on the stability of the diode laser. The signal was filtered with a band-pass filter (10–100 kHz). Filtering slightly distorted the line shapes and shifted the absolute peak frequencies ~0.0036 cm⁻¹; however, the relative frequencies remained unaffected. The final spectrum was recorded between 2340.1 and 2349.9 cm⁻¹. A germanium Etalon temperature stabilized to within 0.06 °C with an average free spectral range of 0.016 cm⁻¹ was used to obtain the relative frequencies. A reference cell containing trace amounts of CO₂ was used to determine the absolute frequencies in the dimer spectrum. All three signals were recorded simultaneously with three transient digitizers, and the results were stored in a computer.

Spectrum Analysis and Structure

About 150 spectral lines that could be ascribed in the spectrum of CO₂-CS₂ were observed between 2344.2 and 2349.9 cm⁻¹. Other spectral features, presumably belonging to another species, were observed below 2344 cm⁻¹. All features in these regions were observed only when CO₂ and CS₂ were both present. The (CO₂)₂ lines were absent throughout much of the CO₂-CS₂ spectrum, but began appearing above 2349 cm⁻¹. The most obvious spectral features of the dimer spectrum were a strong broad peak at 2354.5 cm⁻¹, an order of magnitude more intense than the next most intense transition, and a number of transitions with equal spacings of ~0.08 cm⁻¹ and ~0.17 cm⁻¹ (cf. Figure 1).

Initially we assumed the structure would be slipped parallel like other isoelectronic dimers. Thus, we expected *a*- and *b*-type transitions, with *b*-type spacings of ~2 Å between consecutive *R**R* or *P**P* branch origins and ~(*B* + *C*) spacing between consecutive transitions within the branches. Using a computer program based on the Watson Hamiltonian³⁹

$$H_{\text{rot}} = AJ_a^2 + (B + C)(J^2 + J_a^2)/2 + (B - C)(J_+^2 + J_-^2)/4 - D_J J^4 - D_{JK} J^2 J_a^2 + D_K J_a^4 + \delta_J J^2 (J_+^2 + J_-^2) + \delta_K (J_+^4 + J_-^4) \quad (1)$$

nine *R**R* and *P**P* branches were assigned with consecutive *K*_{*a*}. A

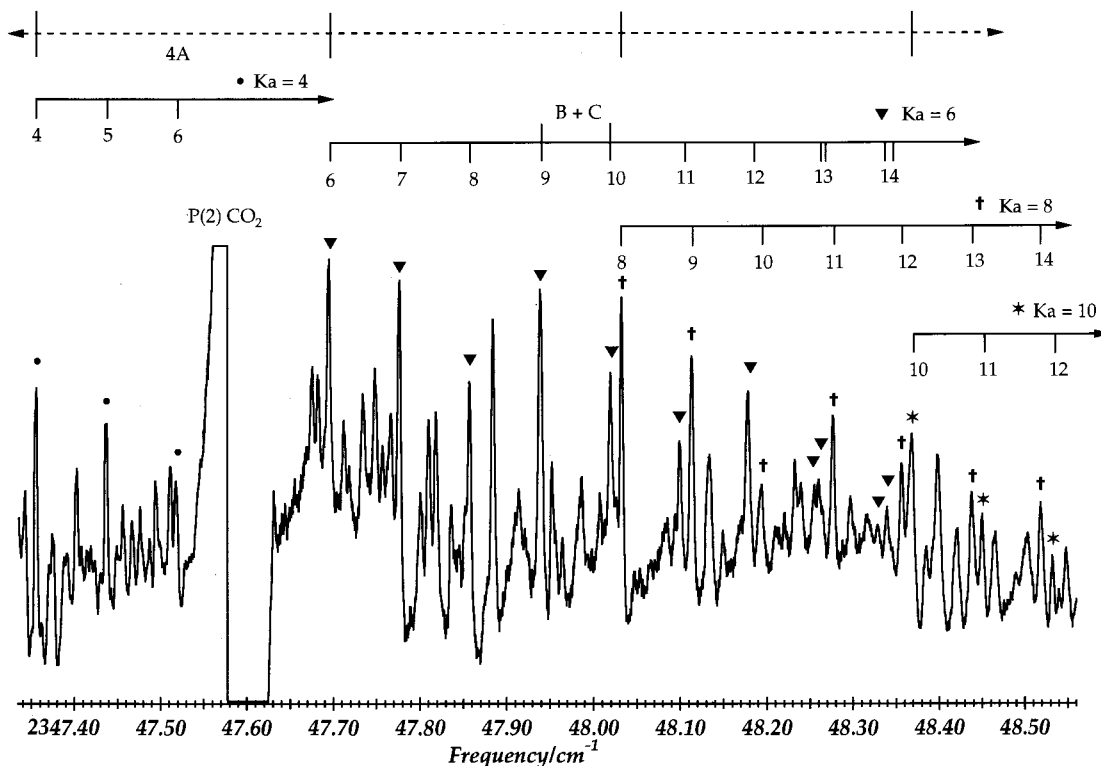


Figure 1. A portion of the R branches of $\text{CO}_2\text{-CS}_2$ dimer between 2347.33 and 2348.55 cm^{-1} . Only even K_a bands are observed. The broad feature between 2347.55 and 2347.63 cm^{-1} is the $P(2)$ transition of the CO_2 monomer.

reasonable fit was obtained for the first five J lines in a band. However, the higher J lines did not agree with predictions even when centrifugal distortions constants were included. Also, the large spectral feature at 2354.5 cm^{-1} , which was presumed to be an a -type Q -branch, was not exactly in the center of the spectrum as predicted and a -type P and R transitions were not observed. Furthermore, the relationships between the rotational constants were inconsistent with a planar structure and the A constant was not of the magnitude expected for a slipped parallel structure.

Next, we considered that the structure might have C_{2v} symmetry allowing the oxygen atoms, as well as the sulfur atoms, to be equivalent. Then, nuclear spin statistics would cause only even K_a bands to be observed spectroscopically. The three types of structures that would have C_{2v} symmetry would be two T-shaped, a planar parallel, and a nonplanar X-shaped configuration. Spectral simulations were carried out in each case. The T-shaped configurations were rapidly rejected. The T-shaped structure with CO_2 on top of the T would allow only b -type transitions to be observed, which would not explain the large central feature. The T-shaped configuration with CS_2 on top would allow only a -type transitions of which none were found. For an X-shaped structure, the selection rules would depend on the dihedral angle, φ . If φ were zero, then the molecule would be planar and only b -type selection rules would be allowed. If the dihedral angle were 90° , then only c -type selection rules could occur. For intermediate dihedral angles, both b - and c -type transitions would exist. Only the c -type selection rules accounted for the large Q -branch in the center of the spectrum at 2354.5 cm^{-1} (cf. Table 2) as well as the several equally spaced series that were present. Finally, 111 lines were fit with a c -type spectrum, and no b -type transitions could be observed. The absence of b -type transitions ruled out a $\text{CO}_2\text{-CS}_2$ geometry with a dihedral angle far from 90° . The experimentally determined constants are shown in Table 3. The centrifugal distortion constants, D_j , D_{jk} , and D_k , were used in

the fit; however, the δ_j and δ_k terms did not improve the fit and were omitted. It was assumed that the monomer structures remained unchanged upon complexation.

An orthogonal orientation of the two monomers can be further substantiated by calculating the planar moments defined as

$$2P_c = I_a + I_b - I_c = 2 \sum_i m_i c_i^2 + \Delta_{ab} \quad (2a)$$

$$2P_b = I_a + I_c - I_b = 2 \sum_i m_i b_i^2 + \Delta_{ac} \quad (2b)$$

where P_c and P_b are the planar moments in the c - and b -directions, respectively, a , b , and c are coordinates in the principal axis frame, and Δ_{ab} and Δ_{ac} are the small discrepancies that would be equivalent to the inertial defect in a planar molecule. The experimental value of P_c (85.5 amu \AA^2) is twice the value of I_{CO_2} (43.2 amu \AA^2). Similarly, P_b is 307.1 amu \AA^2 , which is twice the value of I_{CS_2} (154.5 amu \AA^2). The values 0.9 and 1.9 amu \AA^2 found for Δ_{ab} and Δ_{ac} , respectively, are of the same magnitude as inertial defects found in weakly bound planar complexes (cf. Table 1). Thus, CO_2 and CS_2 are perpendicular, or nearly perpendicular, to each other.

The center-of-mass distance between CO_2 and CS_2 can be determined by

$$R_{cm} = \sqrt{\frac{I_c - I_{\text{CS}_2}}{\mu}} = \sqrt{\frac{I_b - I_{\text{CO}_2}}{\mu}} \quad (3)$$

where I_c and I_b are the component moments of inertia of the dimer, I_{CS_2} and I_{CO_2} are the monomer moments of inertia. The reduced mass, μ , is defined as

$$\mu = \frac{M_{\text{CO}_2} M_{\text{CS}_2}}{M_{\text{CO}_2} + M_{\text{CS}_2}} \quad (4)$$

TABLE 2: Assigned Transitions for the CO₂-CS₂ Dimer

$\Delta K_a \Delta J_{K_a}$	J'	K_a'	K_c'	J''	K_a''	K_c''	expt freq (cm ⁻¹)	expt calc	$\Delta K_a \Delta J_{K_a}$	J'	K_a'	K_c'	J''	K_a''	K_c''	expt freq (cm ⁻¹)	expt calc
${}^R R_2$	3	3	1	2	2	1	2347.0151	0.0004	${}^P P_4$	5	1	5	6	2	5	2345.8405	0.0004
	4	3	2	3	2	2	2347.1006	0.0010		6	1	5	7	2	5	2345.7980	-0.0005
	5	3	2	4	2	2	2347.1676	0.0002		7	1	7	8	2	7	2345.6158	0.0004
	5	3	3	4	2	3	2347.1864	-0.0009		7	1	6	8	2	6	2345.6828	-0.0004
	6	3	4	5	2	4	2347.2779	-0.0009		8	1	8	9	2	8	2345.4992	-0.0004
	6	3	3	5	2	3	2347.2421	0.0005		8	1	7	9	2	7	2345.5599	-0.0000
	7	3	4	6	2	4	2347.3187	0.0000		9	1	8	10	2	8	2345.4331	0.0003
	7	3	5	6	2	5	2347.3741	-0.0004		3	3	0	4	4	0	2345.9010	0.0001
	8	3	6	7	2	6	2347.4736	-0.0012		4	3	1	5	4	1	2345.8180	-0.0011
	8	3	5	7	2	5	2347.4030	0.0006		4	3	2	5	4	2	2345.8180	0.0002
	9	3	6	8	2	6	2347.4939	-0.0010		5	3	3	6	4	3	2345.7345	0.0002
	11	3	8	10	2	8	2347.7120	-0.0000		6	3	4	7	4	4	2345.6490	-0.0001
${}^R R_4$	11	3	9	10	2	9	2347.8008	0.0009	6	3	3	7	4	3	2345.6630	0.0005	
	12	3	10	11	2	10	2347.9142	0.0005	7	3	4	8	4	4	2345.5897	0.0000	
	5	5	1	4	4	1	2347.3544	-0.0003	8	3	6	9	4	6	2345.4716	0.0007	
	6	5	2	5	4	2	2347.4368	0.0000	8	3	5	9	4	5	2345.5189	0.0000	
	7	5	3	6	4	3	2347.5187	0.0000	9	3	6	10	4	6	2345.4451	-0.0007	
	9	5	4	8	4	4	2347.6759	0.0004	10	3	8	11	4	8	2345.2756	-0.0006	
	9	5	5	8	4	5	2347.6829	-0.0001	10	3	7	11	4	7	2345.3658	-0.0003	
	10	5	6	9	4	6	2347.7665	-0.0000	5	5	1	6	6	1	2345.5548	0.0002	
	11	5	7	10	4	7	2347.8523	0.0001	6	5	2	7	6	2	2345.4719	-0.0002	
	${}^R R_6$	7	7	1	6	6	1	2347.6952	0.0009	7	5	3	8	6	3	2345.3900	0.0000
		8	7	2	7	6	2	2347.7765	0.0004	8	5	4	9	6	4	2345.3075	-0.0003
		9	7	3	8	6	3	2347.8575	-0.0001	9	5	4	10	6	4	2345.2275	0.0000
10		7	4	9	6	4	2347.9390	0.0001	11	5	6	12	6	6	2345.0719	0.0001	
11		7	5	10	6	5	2348.0198	-0.0000	12	5	8	13	6	8	2344.9788	-0.0001	
12		7	5	11	6	5	2348.0993	-0.0004	12	5	7	13	6	7	2344.9992	-0.0000	
13		7	6	12	6	6	2348.1783	-0.0004	13	5	8	14	6	8	2344.9320	0.0003	
14		7	7	13	6	7	2348.2551	-0.0008	14	5	9	15	6	9	2344.8678	0.0002	
14		7	8	13	6	8	2348.2601	-0.0006	7	7	1	8	8	1	2345.2070	-0.0001	
${}^R R_8$		9	9	1	8	8	1	2348.0325	0.0000	8	7	2	9	8	2	2345.1248	-0.0000
		10	9	2	9	8	2	2348.1135	-0.0004	9	7	3	10	8	3	2345.0429	0.0002
		12	9	4	11	8	4	2348.2765	0.0000	10	7	4	11	8	4	2344.9611	0.0003
	13	9	5	12	8	5	2348.3560	-0.0012	11	7	5	12	8	5	2344.8797	0.0006	
	14	9	6	13	8	6	2348.4379	0.0000	12	7	6	13	8	6	2344.7981	0.0005	
	15	9	7	14	8	7	2348.5185	0.0004	13	7	7	14	8	7	2344.7160	-0.0006	
	16	9	8	15	8	8	2348.5977	-0.0001	14	7	8	15	8	8	2344.6362	0.0000	
	18	9	9	17	8	9	2348.7550	0.0003	9	9	1	10	10	1	2344.8588	0.0000	
	${}^R R_{10}$	11	11	0	10	10	1	2348.3689	-0.0006	10	9	2	11	10	2	2344.7772	0.0005
		12	11	1	11	10	2	2348.4499	-0.0007	11	9	3	12	10	3	2344.6938	-0.0008
		13	11	2	12	10	3	2348.5320	0.0003	12	9	4	13	10	4	2344.6125	-0.0002
		14	11	3	13	10	4	2348.6124	-0.0001	13	9	5	14	10	5	2344.5310	-0.0001
15		11	4	14	10	5	2348.6932	0.0000	14	9	6	15	10	6	2344.4499	0.0001	
16		11	5	15	10	6	2348.7735	-0.0000	4	1	4	4	0	4	2346.5558	-0.0003	
17		11	6	16	10	7	2348.8536	-0.0000	8	1	8	8	0	8	2346.5429	-0.0002	
18		11	7	17	10	8	2348.9333	-0.0001	9	1	9	9	0	9	2346.5429	0.0006	
19		11	8	18	10	9	2349.0124	-0.0004	6	3	3	6	2	5	2346.8138	0.0004	
${}^R R_{12}$		13	13	0	12	12	1	2348.7056	0.0001	6	1	5	6	2	5	2346.4982	-0.0009
		14	13	1	13	12	2	2348.7863	0.0000	7	1	6	7	2	6	2346.5149	-0.0004
		15	13	2	14	12	3	2348.8672	0.0003	6	3	4	6	4	2	2346.2297	0.0003
	16	13	3	15	12	4	2348.9472	-0.0001	7	3	5	7	4	3	2346.2238	0.0000	
	17	13	4	16	12	5	2349.0280	0.0004	8	3	6	8	4	4	2346.2107	-0.0000	
${}^P P_2$	1	1	0	2	2	0	2346.2489	-0.0005	5	5	1	5	4	1	2346.9410	-0.0003	
	1	1	1	2	2	1	2346.2408	0.0002	8	5	4	8	4	4	2346.9267	0.0006	
	2	1	1	3	2	1	2346.1710	-0.0000	10	5	6	10	4	6	2346.8897	0.0003	
	4	1	4	5	2	4	2345.9474	0.0001									

where M_{CO_2} and M_{CS_2} are the monomer masses. Thus, R_{cm} has been determined to be 3.392 Å.

Modeling the Structure

This geometry has not previously been observed for dimers of linear triatomics, so potential energy calculations were performed to better understand the intermolecular interactions in this system. A number of authors have considered the structures of van der Waals dimers in light of intermolecular interactions, with potentials derived in part from other experiments. A seminal effort is that of Buckingham and Fowler⁴⁰ on the N₂-CO₂ dimer. Closely related to this work is Muentert's⁴¹ study of (CO₂)₂, CO₂-HCCH, and (HCCH)₂

structures, where he assumed Lennard-Jones atom-atom potentials and an electrostatic interaction involving distributed multipoles on the molecules of the dimer. His results give a good understanding of the difference in structure of these dimers.

We have chosen to model the CO₂-CS₂ dimer structure using intermolecular potentials found suitable to explain the properties of molecular crystals of CO₂ and CS₂. We use an atom-atom potential plus point quadrupoles on the molecules as the simplest realistic approach, with the objective of understanding the difference between the slipped-parallel CO₂ dimer and the X-shaped mixed dimer found in this study.

For the atom-atom interactions, a Buckingham potential⁴² (eq 5) was used, requiring three parameters for each type of

TABLE 3: Experimentally Determined Parameters and Structure of CO₂–CS₂^a

parameter	$\nu = 0$	parameter	$\nu = 1$
A''	0.08590 (0.00001)	A'	0.08574 (0.00001)
B''	0.04634 (0.00001)	B'	0.04633 (0.00001)
C''	0.03546 (0.00002)	C'	0.03543 (0.00002)
D_j''	-1.37×10^{-7} (0.65)	D_j'	-1.24×10^{-7} (0.58)
D_k''	1.06×10^{-6} (0.23)	D_k'	1.13×10^{-6} (0.19)
D_{jk}''	-1.01×10^{-6} (0.22)	D_{jk}'	-1.03×10^{-6} (0.19)
I_a''	196.3	I_a'	196.7
I_b''	364.1	I_b'	364.1
I_c''	474.9	I_c'	476.2
R_{cm} (Å)			3.392
κ			-0.57
$\Delta\nu$ (cm ⁻¹)			-2.61

^a Rotational and centrifugal distortion constants are given in cm⁻¹; moments of inertia are given in amu Å²; errors are one standard deviation and shown in parentheses.

interaction: C–C, C–O, C–S, O–S, and O–O (for the CO₂ dimer). The C–C, C–O, and O–O interactions were taken from Procacci et al.,⁴³ who based their results on agreement with physical properties of the CO₂ crystal. We adopted the Buckingham parameters of their potential, PRC-1, which included a set of C–C parameters of Williams.⁴⁴ The C–S (and S–S) parameters were taken from the results of Burgos and Righini⁴⁵ based on similar studies of the CS₂ crystal. The O–S parameters were derived using the conventional combining rules from those for O–O and S–S.

The electrostatic interactions between molecules were represented as those between point quadrupoles (eq 6)⁴² located at the carbon atoms. Both of the studies just mentioned represented the molecular charge distributions by

$$V_{a-a} = \sum_{ij} \left(A_{ij} e^{-B_{ij}R_{ij}} - \frac{C_{ij}}{R_{ij}^6} \right) \quad (5)$$

$$V_{q-q} = \frac{3}{16} \frac{Q_1 Q_2}{R^5} \{ 1 - 5 \cos^2 \theta - 5 \cos^2 \gamma - 15 \cos^2 \theta \cos^2 \gamma + 2(\sin \theta \sin \gamma \cos \varphi - 4 \cos \theta \cos \gamma)^2 \} \quad (6)$$

$$V_{total} = V_{a-a} + V_{q-q} \quad (7)$$

distributed multipoles within the molecules. As a result, there is some inconsistency in our using their Buckingham parameters with a simpler (point quadrupole) electrostatic interaction. Our success in predicting the correct dimer structures and the well-known insensitivity of crystal structure calculations to details of the electrostatic representation gives some justification to this simple approach.

A computer program was written that, starting with an arbitrary assumed structure for the dimer, found the structure of minimum potential energy. The potential parameters used are given in Table 4. Care was taken to ensure that the minimum reached was the one of lowest potential energy if more than one minimum was found.

The CS₂ quadrupole, 3.4×10^{-26} esu cm², and CO₂ quadrupole, -4.3×10^{-26} esu cm² were obtained from Watson and co-workers⁴⁶ from an electric field-gradient-induced birefringence experiment. Previous experiments determining the CS₂ quadrupole resulted in values in agreement with those of

TABLE 4: Parameters Used for the Atom–Atom and Quadrupole–Quadrupole Potential Energy Calculations

atom–atom potential			
atoms	A (kcal mol ⁻¹)	B (Å ⁻¹)	C (kcal Å ⁶ mol ⁻¹)
C–C	83 630	3.600	568
C–O	14 004	3.404	271
C–S	66 000	3.300	1320
O–S	36 000	3.091	1398
O–O	18 300	3.182	637
quadrupole–quadrupole potential			
Θ (esu cm ²)			
CO ₂			-4.3×10^{-26}
CS ₂			$+3.4 \times 10^{-26}$

TABLE 5: Results from Intermolecular Potential Energy Calculations for CO₂–CS₂ and CO₂ Dimer^a

$A-B$	Q_A	Q_B	V_{aa}	V_{qq}	V_{tot}	R_{C-C}	configuration
CO ₂ –CS ₂							
(i)	-4.3	+3.4	-1.317	-0.071	-1.388	3.557	X-shape
(ii)	0.0	0.0	-1.318	0.0	-1.318	3.576	X-shape
(iii)	-4.3	+3.4	+0.079	-0.531	-0.452	3.600	linear
CO ₂ –CO ₂							
(iv)	-4.3	-4.3	-0.589	-0.090	-0.679	3.885	slip parallel
(v)	0.0	0.0	-0.706	0.0	-0.706	3.595	X-shape
(vi)	-4.3	-4.3	-0.005	-0.268	-0.273	3.755	T-shape

^a The potentials used are the Buckingham atom–atom and quadrupole–quadrupole potentials; rows (i) and (iv) show the structure calculated using the complete potential of eq 7; in rows (ii) and (v), the molecular quadrupoles are set to zero; the structures in rows (iii) and (vi) result from quadrupole interactions plus a carbon–carbon potential (see text); quadrupole moments are given in esu cm² ($\times 10^{26}$), V is in kcal/mol and R_{C-C} in Å.

Watson within experimental error and are summarized by de Luca and co-workers.⁴⁷

Results for (CO₂)₂ and CO₂–CS₂ are shown in Table 5, where calculations (i) and (iv) represent the predictions of this theory using the total potential shown in eq 7. In both cases, the structural prediction is in good agreement with experimental results. For (CO₂)₂, a slipped parallel configuration is predicted, with the molecular axes at 63° from the intermolecular vector and an R_{cm} of 3.88 Å (experimental values are 58° and 3.60 Å). For CO₂–CS₂, a perpendicular X-shaped configuration is predicted with R_{cm} of 3.57 Å (experimental value is 3.39 Å).

The energy in each case is dominated by the atom–atom energy. If the molecular quadrupoles are arbitrarily given zero values, both molecules become X-shaped [cf. Table 5, rows (ii) and (v)]. On the other hand, if the atom–atom potentials for all but the C–C interaction are set to zero (the B value for C–C is modified to hold the intermolecular distance to a reasonable value), then the dimers assume expected quadrupole–quadrupole orientations [cf. Table 5, rows (iii) and (vi)]. These structures are T-shaped for (CO₂)₂ (same sign for both quadrupoles) and linear for CO₂–CS₂ (quadrupoles of opposite sign).

Finally, by using the complete potential, if the value of the CS₂ quadrupole increases in magnitude, the dimer shifts from the nonplanar X-shaped structure to a stable planar parallel configuration when the quadrupole reaches $+6 \times 10^{-26}$ esu cm².

In summary, the rovibrational spectrum of CO₂–CS₂ has been obtained indicating the structure is X-shaped (see Figure 2). The vibrationally excited geometry remains virtually unchanged from the ground-state geometry. The atom–atom interactions are responsible for the X-shaped structure. The shape was initially expected to be planar based on the other isolectronic dimers; however, the contribution from the quadrupole moments

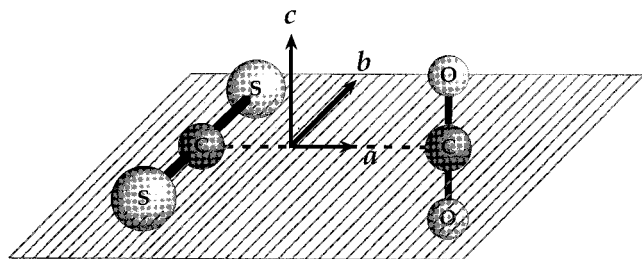


Figure 2. The structure of the CO₂–CS₂ dimer.

is too small to make CO₂–CS₂ planar. Though the multipole interaction energies are weaker than the atom–atom interactions, the orientations of the monomers are controlled by these interactions.

Acknowledgment. We thank the US Army Research Office under the auspices of the Center for the Study of Fast Transient Processes (Grant no. DAAL03-92-G-0175) and the donors of the Petroleum Research fund, administered by the American Chemical Society, for the partial support of this research. In addition, our appreciation goes to Dr. H. Pickett at the Jet Propulsion Laboratories in Pasadena, CA, for use of the SPFIT and SPCAT fitting programs, to Professor T. Miller at The Ohio State University for the use of his SPECSIM simulation program, and to A. Sazonov for some useful discussions.

References and Notes

- Fraser, G. T.; Pine, A. S.; Suenram, R. D.; Dayton, D. C.; Miller, R. E. *J. Chem. Phys.* **1988**, *90*, 1330.
- Baiocchi, F. A.; Dixon, T. A.; Joyner, C. H.; Klemperer, W. J. *Chem. Phys.* **1981**, *74*, 6544.
- Sharpe, S. W.; Zeng, Y. P.; Wittig, C.; Beaudet, R. A. *J. Chem. Phys.* **1990**, *92*, 943.
- Altman, R. S.; Marshall, M. D.; Klemperer, W. J. *J. Chem. Phys.* **1982**, *77*, 4344.
- Lovejoy, C. M.; Schuder, M. D.; Nesbitt, D. J. *J. Chem. Phys.* **1987**, *86*, 5337.
- Zeng, Y. P.; Sharpe, S. W.; Shin, S. K.; Wittig, C.; Beaudet, R. A. *J. Chem. Phys.* **1992**, *97*, 5392.
- Muenter, J. S. *J. Chem. Phys.* **1995**, *103*, 1263.
- Fraser, G. T.; Pine, A. S.; Suenram, R. D. *J. Chem. Phys.* **1988**, *88*, 6157.
- Iida, M.; Ohshima, Y.; Endo, Y. *J. Phys. Chem.* **1993**, *97*, 357.
- Sharpe, S. W.; Sheeks, R.; Wittig, C.; Beaudet, R. A. *Chem. Phys. Lett.* **1988**, *151*, 267.
- Steed, J. M.; Dixon, T. A.; Klemperer, W. J. *J. Chem. Phys.* **1979**, *70*, 4095.
- Weida, M. J.; Spherhac, J. M.; Nesbitt, D. J.; Hutson, J. M. *J. Chem. Phys.* **1994**, *101*, 8351.
- Sazonov, A.; Beaudet, R. A. *J. Phys. Chem.* **1997**.
- Cooke, S. A.; Legon, A. C.; Holloway, J. H. *J. Mol. Struct.* **1997**, *406*, 15.
- Leopold, K. R.; Fraser, G. T.; Klemperer, W. J. *J. Chem. Phys.* **1983**, *80*, 1039.
- Dayton, D. C.; Pedersen, L. G.; Miller, R. E. *J. Chem. Phys.* **1990**, *93*, 4560.
- Walsh, M. A.; Dyke, T. R.; Howard, B. J. *J. Mol. Struct.* **1988**, *189*, 111.
- Legon, A. C.; Suckley, A. P. *J. Chem. Phys.* **1989**, *91*, 4440.
- Block, P. A.; Marshall, M. D.; Pedersen, L. G.; Miller, R. E. *J. Chem. Phys.* **1992**, *96*, 7321.
- Peterson, K. I.; Klemperer, W. J. *J. Chem. Phys.* **1984**, *80*, 2439.
- Jucks, K. W.; Huang, Z. S.; Dayton, D.; Miller, R. E.; Lafferty, W. J. *J. Chem. Phys.* **1986**, *86*, 4341.
- Jucks, K. W.; Huang, Z. S.; Miller, R. E.; G. T. Fraser; Pine, A. S.; Lafferty, W. J. *J. Chem. Phys.* **1988**, *88*, 2185.
- Walsh, M. A.; England, T. H.; Dyke, T. R.; Howard, B. J. *J. Chem. Phys. Lett.* **1987**, *142*, 265.
- Dutton, C.; Sazonov, A.; Beaudet, R. A. *J. Phys. Chem.* **1996**, *100*, 17772.
- Muenter, J. S. *J. Chem. Phys.* **1989**, *90*, 4048.
- Muenter, J. S. *J. Chem. Phys.* **1990**, *94*, 2781.
- Prichard, D. G.; Nandi, R. N.; Muenter, J. S.; Howard, B. J. *J. Chem. Phys.* **1988**, *89*, 1245–1250.
- Novick, S. E.; Suenram, R. D.; Lovas, F. J. *J. Chem. Phys.* **1987**, *88*, 687.
- Blake, T. A.; Novick, S. E.; Lovas, F. J.; Suenram, R. D. *J. Mol. Spec.* **1992**, *154*, 72.
- Bemish, R. J.; Block, P. A.; Pedersen, L. G.; Miller, R. E. *J. Chem. Phys.* **1995**, *103*, 7788.
- Fraser, G. T.; Leopold, K. R.; Klemperer, W. J. *J. Chem. Phys.* **1984**, *81*, 2577.
- Fraser, G. T., Jr.; Charo, A.; Klemperer, W. J. *J. Chem. Phys.* **1984**, *82*, 2535.
- Rice, J. K.; Coudert, L. H.; Matsumura, K.; Suenram, R. D.; Lovas, F. J.; Stahl, W.; Pauley, D. J.; Kukolich, S. G. *J. Chem. Phys.* **1990**, *92*, 6408.
- Bumgarner, R. E.; Pauley, D. J.; Kukolich, S. G. *J. Chem. Phys.* **1987**, *87*, 3749.
- Sun, L.; Ioannou, I. I.; Kuczkowski, R. *Mol. Phys.* **1996**, *88*, 255.
- Huang, Z. S.; Miller, R. E. *J. Chem. Phys.* **1988**, *89*, 5408.
- Hoffbauer, M. A.; Liu, K.; Glese, C. F.; Gentry, W. R. *J. Phys. Chem.* **1983**, *87*, 2096.
- Randall, R. W.; Wilkie, J. M.; Howard, B. J. *Mol. Phys.* **1989**, *69*, 839.
- Watson, J. K. G. *J. Chem. Phys.* **1967**, *46*, 1935.
- Buckingham, A. D.; Fowler, P. W. *Can. J. Chem.* **1985**, *63*, 2018.
- Muenter, J. S. *J. Chem. Phys.* **1991**, *94*, 2781.
- Hirschfelder, J. O.; Curtiss, C. F.; Bird, R. B. *Molecular Theory of Gases and Liquids*; John Wiley & Sons: New York, 1964.
- Procacci, P.; Righini, R.; Califano, S. *Chem. Phys.* **1987**, *116*, 186.
- Williams, D. E. *J. Chem. Phys.* **1967**, *47*, 4680.
- Burgos, E.; Righini, R. *Chem. Phys. Lett.* **1983**, *96*, 584.
- Watson, J. N.; Craven, I. E.; Ritchie, G. L. D. *Chem. Phys. Lett.* **1997**, *274*, 1.
- deLuca, G.; Russo, N.; Sicilia, E.; Toscano, M. *J. Chem. Phys.* **1996**, *105*, 3206.